

POLAR CODE SIMULATION OF DMSP SATELLITE AURORAL CHARGING

David L. Cooke,
M. S. Gussenhoven, David A. Hardy,
Air Force Geophysics Laboratory, Hanscom AFB, MA, 01731

Maurice Tautz, Radex Inc, Bedford MA, 01731

Ira Katz, Gary Jongeward, John R. Lilley Jr.,
Scubed, LaJolla CA, 92038

A study of the charging of the DMSP satellites by auroral electrons is conducted by comparison of numerical simulation, POLAR code, with observations of charging on the DMSP-F6 and F7 spacecraft. These observations have shown that the combined condition of low plasma density and high electron flux will allow charging, with a maximum reported spacecraft ground potential about -1.5 kV. POLAR is a three dimensional Fortran code that solves the Poisson-Vlasov system for self-consistent steady state plasma density and currents around a charged spacecraft. Comparisons have been made between POLAR results and three observations representing distinct parameter regimes. For the one observation where environmental parameters were within POLAR's nominal capabilities, the modeled frame potential of -220 Volts, agreed very well with the observed -215 Volts. Two other observations were chosen to test POLAR on its limits for low plasma density, and low potential charging; producing bad and reasonable agreement respectively. Code results also show significant differential charging due to ram-wake effects, and an effect of spacecraft size and design on charging.]

1. Introduction

The charging of satellites in polar orbit by auroral electrons has been a topic of interest and debate for some time. The relative high density of the Low Earth Orbit (LEO) plasma originally led some to believe that LEO charging would be negligible compared to that observed in Geostationary Orbit (GEO). This early anticipation has been confronted by direct observation of hundreds of volts of negative charging on both the DMSP-F6 and -F7 spacecraft [Besse, & Gussenhoven et.al., 85] with a maximum of -1.5 kV observed so far (unreported observation). Although this is

less than the charging levels observed at GEO, it is significant, and the possibility for higher levels of charging on other systems cannot be precluded without reference to some model or theory.

The Air Force Geophysics Laboratory has sponsored the development of a charging analysis code, POLAR (POtential of Large Spacecraft in the Auroral Region), to specifically study auroral charging. It is essential that any model or theory be tested against observation, and the DMSP data is an obvious choice for comparison with POLAR. This comparison is important for the validation of POLAR, but also for advancing

our understanding the mechanisms of spacecraft charging. The DMSP observations have shown that combinations of high flux and low background density will lead to charging, but do not tell us much about such factors as composition, shape or size.

II. Observations

The DMSP F6 satellite was launched on December 20, 1982 into a sun synchronous, dawn-dusk, circular orbit at an altitude of 840 km, orbital period of 101.5 min, and an inclination of 99°. The DMSP F7 satellite was launched in November, 1983, into a similar orbit in the 1030-2230 magnetic local time (MLT) meridian. The two satellites each carry the SSJ/4 instrument which measures precipitating ions and electrons, and the SSIE instrument, which measures thermal plasma.

The SSJ/4 sensor consists of four cylindrical curved plate electrostatic analyzers arranged in two pairs. One pair measures electron fluxes in 20 logarithmically spaced energy channels between 30 eV and 30 keV, executing a complete sweep each second. The other measures ions over the same range. The analyzer apertures always face local vertical, and thus measure only the precipitating particle populations with an angular acceptance of $10^\circ \times 10^\circ$.

The thermal plasma detector, SSIE consists of a spherical Langmuir probe to measure thermal electrons and a planar retarding potential analyzer, RPA, to measure thermal ions. The Langmuir probe consists of a 1.75 inch diameter collector surrounded by a concentric wire mesh grid of 2.25 inch diameter. It is mounted at the end of a 2.5 foot rigid boom. Complete descriptions of the SSIE instruments, modes of operations, and data analysis methods are

given in *Smidty et al.*, [1978]. From the SSIE data, the thermal plasma density can be determined.

The observations are summarized in Table 1, taken from *Gussenhoven et al.*, [1985], where it was demonstrated that the occurrence and level of charging are well correlated with the ratio of electron flux with energy greater than 14 keV divided by the ambient plasma density ($\text{IF}(\geq 14 \text{ keV})/n_{th}$). They also present other evidence to established that these events do indeed correspond to the passage of the satellites through visibly bright auroral arcs.

III. The POLAR Code

POLAR [*Lilley et al.*, 1985] is a self-consistent three dimensional Poisson-Vlasov code, that provides steady state solutions by iterating between potential (Poisson) and density (Vlasov) solutions on a cubical mesh. A versatile set of building elements can be combined to form complex objects with a variety of surface materials and electrical connections. A surface charging module can be added to the iteration to provide the spacecraft charging response to both natural and active charge drivers. The Poisson solver uses a finite element conjugate gradient method, with a unique technique of filtering charge densities to suppress grid noise, and produce stable solutions. POLAR calculates particle densities by a method that divides space into (one or more) sheath and non-sheath regions separated by a sheath edge(s), located as an equi-potential, near kT . External to this surface the plasma distribution is presumed to be Maxwellian with possible flow. External densities are determined by geometric ray tracing with first order electric field corrections. This approach has been shown to correctly predict wake formation about the Space Shuttle Orbiter [*Murphy et al.*, 1987]. At the sheath

TABLE 1. Summary of 11 Charging Events in 1983. [Gussenhoven et al., 1985]

Satellite	Day	Year	UT _{max} s	Δt s	-φ _{max} ^a V	n ₀ (Ions) cm ⁻³	IF _T (Electrons) (cm ⁻² s sri) ⁻¹	IF (≥ 14 keV) (Electrons) (cm ⁻² s sri) ⁻¹	IF (Ion Peak) (Ions) (cm ⁻² s sri) ⁻¹
F6	Jan 9	1983	49.480	24	213	2.57 × 10 ³	1.43 × 10 ⁹	1.20 × 10 ⁸	3.12 × 10 ⁹
F6	Jan 10	1983	74.722	12	68	1.34 × 10 ⁴	3.79 × 10 ⁹	2.11 × 10 ⁷	3.93 × 10 ⁹
F6	Jan 12	1983	15.377	17	462	5.37 × 10 ²	1.02 × 10 ¹⁰	9.40 × 10 ⁷	4.53 × 10 ⁷
F6	Jan 20	1983	50.047	3	679	3.49 × 10 ²	5.86 × 10 ¹⁰	6.24 × 10 ⁷	3.34 × 10 ⁹
F6	Jan 21	1983	54.937	12	100		1.32 × 10 ⁹	1.49 × 10 ⁹	5.26 × 10 ⁹
F6	Nov 26	1983	47.712	18	317		1.32 × 10 ¹⁰	4.58 × 10 ⁷	1.79 × 10 ⁹
F6	Nov 26	1983	66.068	16	462		1.67 × 10 ⁹	4.79 × 10 ⁷	2.20 × 10 ⁹
F7	Nov 26	1983	43.841	4	47	1.25 × 10 ³	7.36 × 10 ⁸	5.37 × 10 ⁸	1.73 × 10 ⁷
F7	Nov 26	1983	49.843	60	314	1.25 × 10 ²	1.59 × 10 ⁹	1.14 × 10 ⁹	2.07 × 10 ⁹
F7	Dec 01	1983	1.458	2	215	3.55 × 10 ³	2.37 × 10 ⁹	1.95 × 10 ⁹	3.01 × 10 ⁷
F7	Dec 31	1983	14.007	62	462	1.22 × 10 ³	2.39 × 10 ⁹	2.23 × 10 ⁹	1.48 × 10 ⁹

^aThe parameter φ_{max} is inferred from the central energy E_c of the ion energy channel in which the charging peak is identified. ΔE/E_c is 9.3% for both DMSP F6 and F7.

edge reasonable assumptions about the external potential structure and the usual constants of motion are used to determine the flux and velocity of ions entering the sheath which are assigned to a super-particle and tracked inward. Internal sheath densities are determined from the time spent in each volume element, and surface currents from their final deposition. When particles are repelled, their density is assumed to be Boltzmann.

Auroral electrons are introduced with three distinct energetic populations [Fontheim, 1982]: Power Law, specified by intensity, exponent, lower and higher cutoffs; Maxwellian, specified by density and temperature; Gaussian, specified by intensity, energy peak, and peak width. Auroral electrons are assumed to not contribute significant space charge so they are decoupled from the P-V portion of the iteration. They and other sources of current are accounted for during a charging step which updates conductor and surface potentials. The Auroral electron flux is assumed to be isotropic, with no surface - surface shadowing, and secondary and backscatter currents are determined from surface potential and material properties [Katz, 1986]. The isotropy assumption is a

limitation on accuracy, and could be straightforwardly removed, but remains since 4π observations are not usually available, and since a charging code is often used for 'worst case' analysis. Photo electron currents are also included, with shadows calculated from sun direction information.

In modeling DMSP, POLAR is hampered by its single sized grid structure. In designing POLAR to model the Shuttle Orbiter in the 200 - 400 km altitude range, with an ambient plasma density range of 10³ < N_e < 10⁷ cc⁻¹, 10 > λ_D > 0.1 cm, it was decided that a single grid would be adequate for shuttle, sheaths, and scope of project. A plasma sheath thickness will always be bounded by the planar Child-Langmuir length, D_{CL} = λ_D (eV / kT)^{3/4}, which will always be comparable to the shuttle scale. DMSP orbits at 840 km, where the plasma density varies from 10 < N_e < 10⁵ cc⁻¹, 100 > λ_D > 1 cm. With a satellite size of approximately 2 meters, hundred volt sheaths in the low density extreme will become much larger than the satellite. If we choose a fine resolution of the satellite, the total number of nodes will increase run times to prohibitive levels (the high resolution DMSP model at UT1458 employed 2.5 × 10⁵ nodes and required about

200 hours at 10^6 flops). POLAR manages memory better than it does time by maintaining a data base on disk and paging fragments of the problem into core so the largest problems can be run on small high performance workstations. POLAR does not require that the Debye length be resolved as is common in explicit particle simulations. Because of a technique called Charge Stabilization [Cooke et al., 1985], the grid interval can be very large with respect to λ_D without Poisson instability, but sheaths do tend to expand since in reality the sheath edge has λ_D scale structure which expands to the grid interval. With an inflated sheath comes higher sheath currents.

The large DMSP sheaths are also a problem for POLAR's sheath current and density algorithm. In the space charge limited regime where sheath thickness is less than or comparable to object size, angular momentum effects on the trajectories of incoming ions can be reasonably modeled with a single super-particle at each sheath element. For large sheaths, this friendly feature is lost. In a stationary plasma, one can appeal to the analytic orbit-limited limit [Laframboise and Parker, 1973], but in LEO, the orbital momentum of the incoming ions is not only high, its not even spherically symmetric. In the course of the DMSP study, the POLAR sheath model was extended to optionally replace a single sheath particle with a distribution of 5 particles that better samples the momentum of the incoming particles.

In the low density extreme, it would appear desirable to abandon particle tracking. Inspection of large sheath particle tracks in POLAR models reveals very chaotic orbital motion, and surface deposition patterns, that can be quite sensitive to initial conditions. Since it is not practical to approach problems with an ensemble of variant calculations, one

is inclined to give up the pursuit of surface level accuracy for a more efficient approach to the bulk charging. On a trial basis, we have introduced an ad hoc 'Orbit Limited' type model, where we seek a formula for the net surface current as an analytic function of potential, similar to the successful approach employed by NASCAP [Katz, 1978]. This formula gives for surface current density,

$$J = J_{th} \left\{ 1 + \sqrt{\frac{\pi}{8}} M \right\} \left\{ 1 - eV/kT \left[1 + M^2 \right] \right\}$$

$$, J_{th} = \sqrt{kT/2\pi m}, M = \text{velocity} \sqrt{m_i/kT}$$

The second term in the first braces is the ram current to a disk assuming a thermal current to a sphere. The second term in the second braces converts the orbit limited temperature to the flow energy.

POLAR is also challenged by small potentials. The Poisson solver is not bothered, but when surfaces have potential near kT , zero, or $M^2 kT/2e$, currents can be difficult to calculate, particularly near higher surface and space potentials.

IV. Satellite Models

The observations presented in table 1 represent a very wide range of parameters. Some of these cannot be reasonably modeled with POLAR, due to constraints posed by the combination of density and potential. For example, the F6 observations on Jan. 12 & 20, indicate high level charging with low ambient density. These conditions will produce a very extended sheath, which is difficult to model for the reasons presented in the previous section. Reducing the object and grid resolution can help, and in this study, two different resolution DMSP satellite models have been used. These models and the distribution of materials were derived from satellite documentation [DMSP, 1983], and from a cardboard, CAE model of DMSP

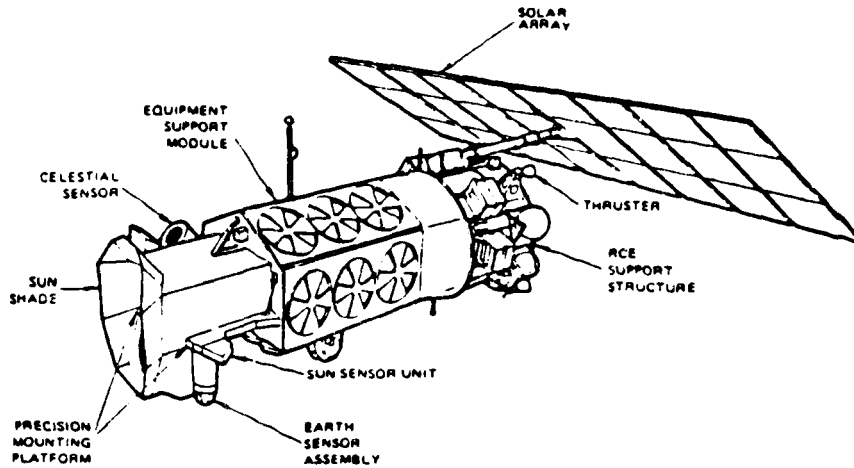


Figure 1. Illustration of DMSP [DMSP, 1983]

provided by RCA Astro Div. (now GE Astro Space Div.). A sketch of DMSP from the documentation with a few features is shown in figure 1. The high resolution POLAR model is shown viewed from ram and wake in figures 2 and 3 along with material designations.

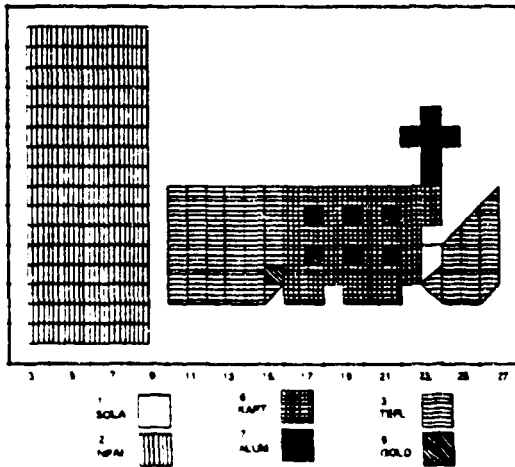


Figure 2. Surface cell material composition as viewed from the + X direction.

The gold patch on the ram side represents the location of the SSIES RPA on later versions of DMSP. The SSIE RPA for F6 and F7 is the round disk located on the boom just above the satellite in figure 1. It is too small to be separately modeled with POLAR. The cross structure above the satellite in figure 2

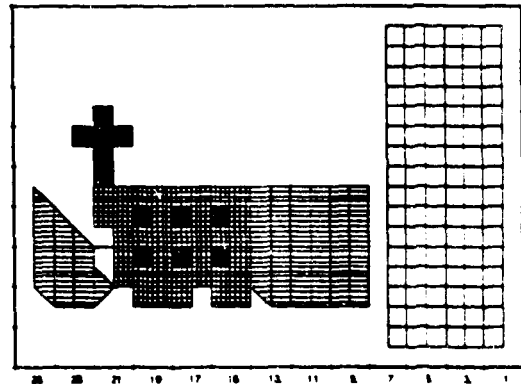


Figure 3. Surface cell material composition as viewed from the - X direction.

represents a microwave imaging sensor (actually round), found on some versions of DMSP. All material were chosen from the default list of POLAR (NASCAP) materials, which in some cases are guesses. The worst guesses are probably the non-conducting paint used on the back side of the solar cells, and the assumption that the aluminized backing of the teflon and kapton thermal blankets is always uniformly grounded. The solar cells have been modeled as uniform solar cell cover glass. The real mix of glass and conducting interconnects has a complex current collection characteristic that cannot be treated as a simple material. NASCAP/LEO [Mandell, 1986] employs a promising hybrid potential and electric field

dependent material treatment that could be adopted if this appears to be a limiting factor.

V. Comparisons

Three observations were chosen from Table 1 for comparison with POLAR. Charging on F6, Jan. 10, 1983, UT74,722, is chosen because the plasma density and sheath size are reasonable for POLAR, and because the low potential will test POLAR's ability to model threshold charging. Charging on F7, Dec. 01, 1983, UT1,458, is chosen because the charging is significant with a plasma density sufficient to produce a tractable sheath size. Charging on F7, Dec. 31, 1983, UT14,007 produces a impossibly large sheath, but was included as a test of the analytic Orbit limited ion model. These events are hence tagged by their Universal Times.

The first step in developing the POLAR models was fitting the observed electron spectra. For this purpose, representative spectra were chosen from the observations, fitted by the POLAR spectral parameters, and assumed to be constant over the event duration. It would have been preferable to compute the average observed spectra before fitting, but this was not done. Better still would be to introduce new fits to spectra as they varied, but since the fitting is now done by hand and eye, this would have been prohibitively time consuming. Possibly the best approach would have been for POLAR to accept numerical spectra, but presently, that option does not exist.

Figure 4 shows the fit at UT1,458, where the resultant POLAR line and the observation are almost identical. Figure 5 shows the poorest fit which is for UT74,722. The spectra at UT14,007 is similar to UT1,458. Significant uncertainty enters the models with respect to the environments. From the observations, we do not know the electron

population above 30 keV, or the extent outside of the observation solid angle, and the reported ion density can be influenced by space potential focusing effects. In all calculations, the ion density was set to that reported in Table 1, and 0.02 eV was used for the ion temperature.

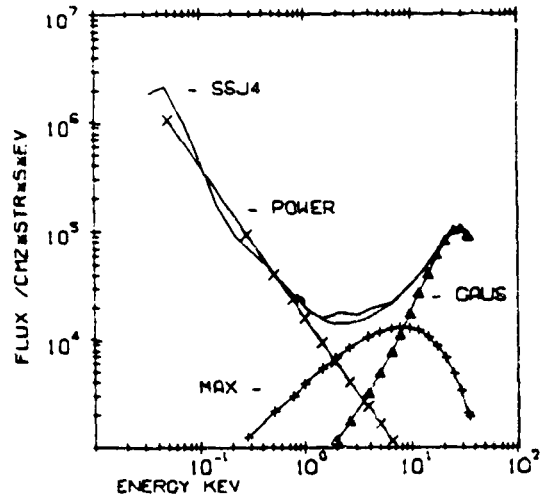


Figure 4. POLAR fit to the F7 SSJ4 spectrum. Observations on Dec 01, 1983, UT 1,458, fitted with Power law, Maxwellian, and Gaussian components.

Charging at UT1,458 and UT74,722 was modeled with both the high resolution DMSP model and DMSPWE. Because of the the compute time required for the high resolution model, large time steps were taken. POLAR's charging algorithm has implicit stability, but the nature of that algorithm in it's implicit limit leaves the temporal fidelity suspect. Therefore, in figure 6, we present the charging history at UT1,458 for the DMSPWE only.

The charging history suggests that the frame potential reaches equilibrium very early with respect to the dielectric surfaces which is as expected since the dielectric to conductor capacitance will be much higher than from the frame to infinity. Given the uncertainties, the close agreement between

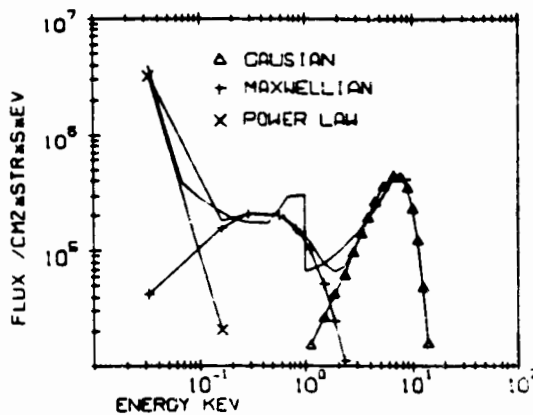


Figure 5. UT 74,722 observation and POLAR fit.

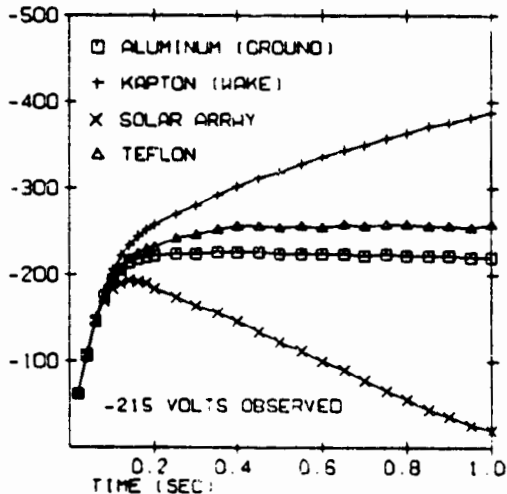


Figure 6. DMSPWE Charging history for selected surfaces at UT 1,458.

this model and observation reflects some degree of luck. Wake side surface potentials for DMSPWE are shown in figure 7, where not surprisingly, the highest potentials are found on the wake side teflon surfaces. For comparison, the high resolution model wake side potentials are shown in figure 8. Here the same teflon surfaces are highly charged, but a few kapton surfaces partially hidden in a cleft have taken the lead. The high res. ram side is presented in figure 9, which exhibits lower potentials because of the ram ion flux. The exception is the edge of the solar array

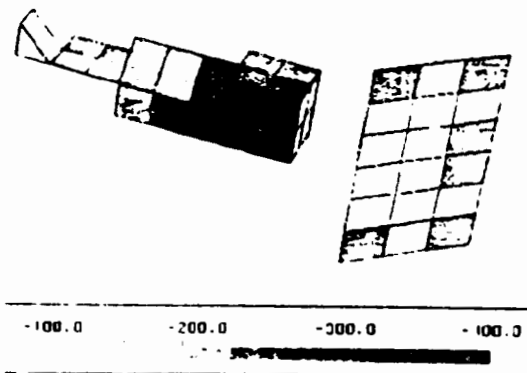


Figure 7. DMSPWE wake side surface potentials

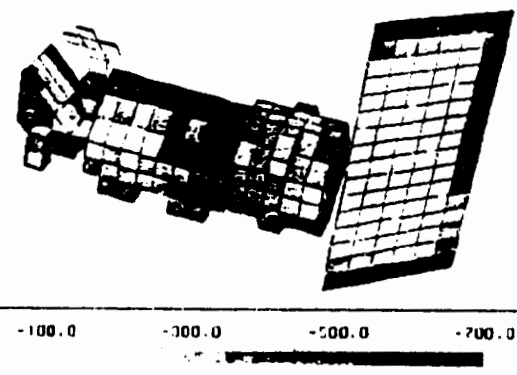


Figure 8. DMSP wake side surface potentials

which charges on both the ram and wake sides. The charging of the ram side of the solar array appears to be an artifact of a surface current smoothing algorithm that has moved some of the ram side current to the back, leaving the ram edge with insufficient ion flux to prevent charging.

Figure 10 is a 2D cut through the 3D POLAR grid showing a shadow outline of the satellite, and space potential contours. The sheath edge used to compute ion fluxes and launch the tracked particles lies at a slightly more negative potential than the kT contour labeled in the figure.

Spacecraft frame potentials calculated by POLAR and observed on DMSP at all three times are summarized in Table 2. In all three cases POLAR and observations are in rough

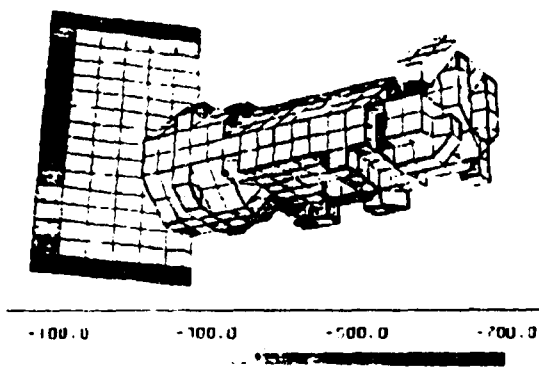
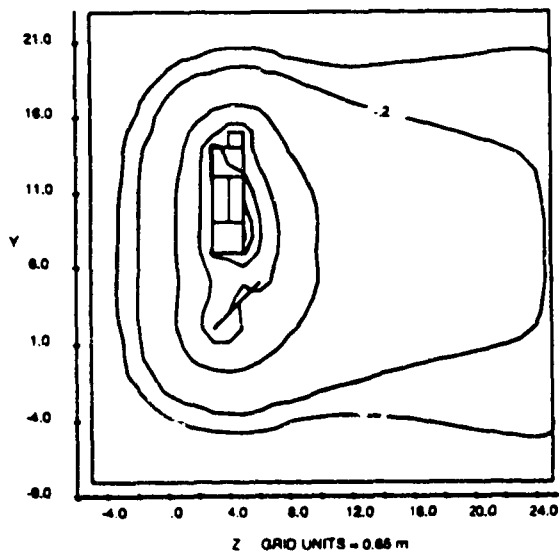


Figure 9. DMSPE ram side surface potentials



Contour Levels, Volts: -300, -200, -100, -20, -0.2, 0.02
Figure 10. Contour plot of DMSPE at UT 1,458.

agreement. The trends are correct, and the values are as close as one can expect given the uncertainty in code physics, environmental uncertainty, and model fidelity.

We may also use POLAR to assess whether additional uncertainty can be attributed to the measurement of ion density. Figure 11 is a plot of ram side ion currents for UT1,458. The ion flux to a square surface of an uncharged satellite would be 2.6×10^{-7} Amp, which would be mostly

Tag	UT1,458	UT14,007	UT74,722
F7 / F6	215	500	68
Polar			
DMSP	390	--	12
DMSPWE	230	1200	11
Big PWE	802	--	--

white in figure 11. As we can see most surfaces collect more.

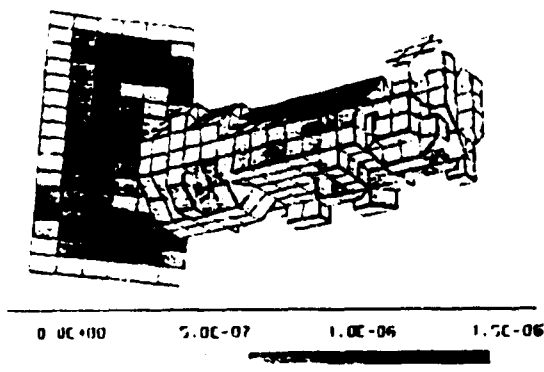


Figure 11. Ram side ion surface currents at UT 1,458.

Without knowledge of the actual focusing factors, which vary with the interaction, it is reasonable to assume no focusing in determining an observed density. ($N = Flux_{observed} / V_{orbit}$) We must however assume that the measured ion density has an interaction induced uncertainty when charging occurs. In fact, if we reduce the ion density in the POLAR UT 74,722 model by a factor of two, the satellite charges to -57 Volts with the ram side focusing factors exceeding 2 for some surfaces.

The differences between the high and low resolution models tell us about the effect of some of the assumptions discussed in section 3. Note that for UT 1,458, the high resolution model charged to the higher potential. The increased variegation on the high res. model without surface shadowing increases the net electron flux. The lower resolution model has slightly higher net ion

fluxes due to sheath thickening effect of the charge stabilization, so in comparison, the high res. has lower fluxes. Both of these effects are of about the same magnitude and contribute to the higher high res. charging.

We can also take this opportunity to take a look at the size effect. In the model listed as "BIG PWE" in table 2, the DMSPWE calculation was rerun with the mesh size parameter increased by a factor of four, which produced an almost four fold increase in charging.

VI. Conclusions

The results and comparisons in this study have shown that POLAR is capable of modeling at least some of the DMSP charging events. This was not a blind study, and for that reason, the conclusions are not as strong as otherwise. Had table 1 been presented to those of us who set up the POLAR runs without the charging levels, most would have been run. Those models with low density and presumably high charging levels would have been abandoned when sheaths grew too large. Although incomplete, runs abandoned due to charging would have strengthened an affirmative assessment of POLAR capability. In the course of pursuing these results a few bugs were fixed, and some extensions were made. The most significant extensions were the 'orbit limited' extension which is mostly a conceptual start, and the thermal sheath particle spreading, which has been of continuing usefulness.

We may also recommend (to ourselves) changes that would improve the code. The surface current spreading should be either eliminated, or made smarter. Wake side charging bleeding onto the ram could be mistaken for a real phenomenon. Although the net ion fluxes are conserved, barrier effects and the secondary currents that might

or might not be suppressed, could depend upon the actual location of surface potential. Incorporating available improvements in solar cell treatment would also be desirable. We also saw how two small effects, artificial sheath current enhancement in low resolution models, and the lack of self-shadowing in auroral electron current deposition, combined to produce a weak scale dependence for charging. While individually small effects, their ability to combine suggests that they are best corrected.

A nested grid capability would definitely enhance POLAR. The large sheath problems would run quicker, but the idea of mapping currents from a sheath edge to surfaces probably breaks at some point which may lie within present capabilities. If one anticipates such a breakdown, it should be addressed before extending POLAR. Another reason for wishing a nested or multi-grid capability, would be the ability to enhance surface resolution. The value here is again subject to the mapping accuracy question, and to limits of the building block approach, which should be updated along with any improvements in gridding.

In conclusion, POLAR, does appear capable of predicting the presence and levels of auroral charging.

References

- Besse, A.L., A.G. Rubin, and D.A. Hardy, "Charging of DMSP/F6 in Aurora on 10 January 1983", in *proc. Spacecraft Environmental Interactions Tech. Conf.* ed. by C.K. Purvis and C.P. Pike, NASA Conf. Pub. 2359, AFGL-TR-85-0018, 1985. ADA202020
- Cocke, D.L., I. Katz, M. Mandell, J.R. Lilley Jr., and A.J. Rubin, "A Three-Dimensional Calculation of Shuttle Charging in Polar Orbit", in *proc. Spacecraft Environmental Interactions Tech. Conf.* ed. by C.K. Purvis and C.P. Pike, NASA Conf. Pub. 2359, AFGL-TR-85-0018, 1985. ADA202020
- DMSP, "Defense Meteorological Satellite Program (DMSP) Block 5D-2 System Analysis Report", Prep.

- by DMSP Prog. Off. RCA Gov. Sys. Div.,
Astro-Electronics, Princeton, NJ., for Space Division
(YD), USAF, Los Angeles, CA, CDRL Item C108,
Contract F04701-75-C-0182, Nov. 1984.
- Fontheim, E.G., K. Stasiewicz, M.O. Chandler,
R.S.B. Ong, E. Gombosi, and R.A. Hoffman,
"Statistical Study of Precipitating Electrons", J.
Geophys. Res., V87, A5, 1982.
- Gussenhoven, M.S., D.A. Hardy, F. Rich, and W.J.
Burke, "High-Level Spacecraft Charging in the
Low-Altitude Polar Auroral Environment", J.
Geophys. Res., Vol.90, No.A11, pp. 11,009-11,023,
Nov. 1985.
- Katz, I., M.J. Mandell, G. Jongeward, M.S.
Gussenhoven, " The Importance of Accurate
Secondary Electron Yields in Modeling Spacecraft
Charging, J. Geophys. Res., V91, No.A12, pp 13,744;
1986
- Katz, I., M.J. Mandell, G.W. Schnuelle, J.J. Cassidy,
P.G. Steen, and J.C. Roche, " The Capabilities of the
NASA Charging Analyzer Program", in proc.
Spacecraft Charging Technology Conference,
AFGL-TR-79-0082, NASA Conference Pub 2071,
1978. ADA084626
- Lilley J.R. Jr., D.L. Cooke, G.A. Jongeward, I. Katz.
"POLAR Users Manual", AFGL-TR-85-0246, 1985. ADA173758
- Laframboise, J.G., and L.W. Parker, "Probe design for
orbit-limited current collection", Physics of Fluids,
V16, #5, May 1973.
- Mandell, M.J., I. Katz, G.A. Jongeward, J.C. Roche,
"Computer simulation of plasma electron collection by
PIXII, J. Spacecraft and Rockets, V23, #5, Sept 1986.
- Murphy, G., and I. Katz, "The POLAR Code Wake
Model: Comparison with in Situ Observations",
J. Geophys. Res., V94, pp. 1,450, 1989.
- Smiddy M., R.C. Sagalyn, W.P. Sullivan, P.J.L.
Wildman, P. Anderson, and F. Rich, "The Topside
Ionosphere Plasma Monitor (SSIE) for the Block
5D/flight 2 DMSP Satellite", Rep.,
AFGL-TR-78-0071, Hanscom AFB, Mass. 1978.
ADA058503